



# FGF2 Affects Parkinson's Disease-Associated Molecular Networks Through Exosomal Rab8b/Rab31

Rohit Kumar<sup>1,2,3\*†</sup>, Sainitin Donakonda<sup>4†</sup>, Stephan A. Müller<sup>1</sup>, Kai Bötzel<sup>3</sup>, Günter U. Höglinger<sup>1,2,5</sup> and Thomas Koeglsperger<sup>1,3\*</sup>

<sup>1</sup> German Center for Neurodegenerative Diseases (DZNE), Munich, Germany, <sup>2</sup> Faculty of Medicine, Klinikum Rechts der Isar, Technical University of Munich, Munich, Germany, <sup>3</sup> Department of Neurology, Ludwig Maximilian University, Munich, Germany, <sup>4</sup> Institute of Immunology and Experimental Oncology, Technical University of Munich, Munich, Germany, <sup>5</sup> Department of Neurology, Hannover Medical School, Hanover, Germany

## OPEN ACCESS

### Edited by:

Anna Marabotti,  
University of Salerno, Italy

### Reviewed by:

David Meckes,  
Florida State University, United States  
Khanh N. Q. Le,  
Taipei Medical University, Taiwan

### \*Correspondence:

Rohit Kumar  
rohit.kumar@dzne.de  
Thomas Koeglsperger  
thomas.koeglsperger@dzne.de

† These authors have contributed  
equally to this work

### Specialty section:

This article was submitted to  
Computational Genomics,  
a section of the journal  
Frontiers in Genetics

Received: 12 June 2020

Accepted: 02 September 2020

Published: 25 September 2020

### Citation:

Kumar R, Donakonda S,  
Müller SA, Bötzel K, Höglinger GU  
and Koeglsperger T (2020) FGF2  
Affects Parkinson's  
Disease-Associated Molecular  
Networks Through Exosomal  
Rab8b/Rab31.  
Front. Genet. 11:572058.  
doi: 10.3389/fgene.2020.572058

Ras-associated binding (Rab) proteins are small GTPases that regulate the trafficking of membrane components during endocytosis and exocytosis including the release of extracellular vesicles (EVs). Parkinson's disease (PD) is one of the most prevalent neurodegenerative disorder in the elderly population, where pathological proteins such as alpha-synuclein ( $\alpha$ -Syn) are transmitted in EVs from one neuron to another neuron and ultimately across brain regions, thereby facilitating the spreading of pathology. We recently demonstrated fibroblast growth factor-2 (FGF2) to enhance the release of EVs and delineated the proteomic signature of FGF2-triggered EVs in cultured primary hippocampal neurons. Out of 235 significantly upregulated proteins, we found that FGF2 specifically enriched EVs for the two Rab family members *Rab8b* and *Rab31*. Consequently, we investigated the interactions of *Rab8b* and *Rab31* using a network analysis approach in order to estimate the global influence of their enrichment in EVs. To achieve this, we have demarcated a protein-protein interaction network (PPIN) for these Rabs and identified the proteins associated with PD in various cellular components of the central nervous system (CNS), in different brain regions, and in the enteric nervous system (ENS). A total of 126 direct or indirect interactions were reported for two Rab candidates, out of which 114 are *Rab8b* interactions and 54 are *Rab31* interactions, ultimately resulting in an individual interaction score (IS) of 90.48 and 42.86%, respectively. Conclusively, these results for the first time demonstrate the relevance of FGF2-induced Rab-enrichment in EVs and its potential to regulate PD pathophysiology.

**Keywords:** Parkinson's disease, exosomes, Rab proteins, membrane-trafficking, vesicular transport

## INTRODUCTION

Parkinson's disease (PD) is a progressive neurodegenerative disorder characterized by the loss of neurons in substantia nigra pars compacta (SNc) and the gradual appearance of intraneuronal protein aggregates, termed Lewy bodies (LBs) (McCann et al., 2016). Neuropathological investigations in PD cases proposed that LBs first appear either in the olfactory bulb (OB) or the

dorsal motor nucleus of the vagus (DMV) in the caudal medulla (Braak et al., 2003b). Prior to central nervous system (CNS) manifestation, Lewy pathology (LP) has therefore been assumed to begin in the gastro-intestinal tract as demonstrated by the presence of Lewy neurites (LNs) in the enteric nervous system (ENS) of PD patients (Holmqvist et al., 2014; Sanchez-Ferro et al., 2015). The gradual appearance of LBs in different brain regions correlates with progressive PD symptoms at distinct disease stages (Braak and Del Tredici, 2017).

Dementia in PD patients is associated to the appearance of LBs in hippocampal neurons together with a decrease in cholinergic transmission (Hall et al., 2014). LBs are largely composed of alpha-synuclein ( $\alpha$ -Syn) and likely result from genetic factors and organelle dysfunction (Shults, 2006). Previous *in vitro* and *in vivo* studies demonstrate that  $\alpha$ -Syn may be transferred from cell to cell, thereby promoting the “spread” of LP between different brain regions (Li et al., 2008; Cavaliere et al., 2017). It has been shown that  $\alpha$ -Syn transfer can further seed the formation of LBs (Jones et al., 2015). Extracellular vesicles (EVs) from patients of dementia with LBs (DLB) enhanced the formation of  $\alpha$ -Syn aggregates in the mouse brain, thus validating the idea of propagation via EV-mediated content exchange (Ngolab et al., 2017). It has been observed that EVs carry pathogenic  $\alpha$ -Syn species to enhance the  $\alpha$ -Syn aggregation process (Grey et al., 2015; Stuenkel et al., 2016). Conversely,  $\alpha$ -Syn is found capable of promoting EV release in CNS cells (Chang et al., 2013). The capacities of  $\alpha$ -Syn to modulate vesicular populations are also known (Dettmer et al., 2017) and mutations of  $\alpha$ -Syn were shown to defect the neuron’s endocytic machinery and impair vesicular transport in neurons, which is an earlier step of EV biogenesis pathway (Volpicelli-Daley et al., 2014; Xu et al., 2016). As a result, early-stage PD pathology exhibits a dysfunction in intracellular trafficking mechanisms (Hunn et al., 2015). Furthermore, it is reported that endoplasmic reticulum (ER)-Golgi vesicle trafficking genes, i.e., Ras-associated binding proteins (Rabs), modulate  $\alpha$ -Syn-induced toxicity and share functional associations with  $\alpha$ -Syn (Cooper et al., 2006; Breda et al., 2015). Rabs in general are one of the most abundant family of proteins and are involved in regulation of cellular functions such as intracellular component trafficking of organelles, proteins, and membranes via their binary mode of activation contingent to GTP/GDP bound states (Villaruel-Campos et al., 2016). In neurons, these Rab-mediated intracellular trafficking is associated to regulate the developmental processes (Shikanai et al., 2018). Processes such as neurodevelopment along with many others are governed via cross-communication among the nervous system (NS) components to which vesicular trafficking is at the center and largely regulated by Rab members (Ng and Tang, 2008). Furthermore, Rabs-mediated regulation of vesicular trafficking involves them to control the mechanisms of synaptic function, therefore making them worthy participants of both normal and disease pathophysiology altogether (Kiral et al., 2018; Mignogna and D’Adamo, 2018), though a comprehensive account of their roles in NS is unavailable. Continuous efforts have been made to classify and determine their functions and mode of actions (Le et al., 2018, 2019).

We recently demonstrated that fibroblast growth factor-2 (FGF2), a modulator of neuronal cholinergic activity, increases the release of EVs (Araujo et al., 1993; Kumar et al., 2020). In this recently published study, we performed mass spectrometry (MS) and found that FGF2 has significantly altered the EV proteome, leading to 441 proteins with a fold change of 1.5 and above. In total, 235 upregulated and 206 downregulated proteins were screened for members of the Rab protein family. We found that FGF2-triggered EVs were specifically enriched for *Rab8b* and *Rab31*. Hence, to further conclude on the global effects of *Rab8b* and *Rab31* enrichment and their importance in PD pathology, we performed protein–protein interaction network (PPiN) analysis and identified their interactions in different CNS-resident cell types, in different brain regions, and in ENS, highlighting the novel role of FGF2 in PD pathophysiology and paving a way forward to investigating the specific role of FGF2 in PD.

## MATERIALS AND METHODS

### EV Proteome From Primary Hippocampal Neurons

All animal experiments were conducted in accordance with the regulations of the local animal welfare committee. Primary hippocampal neurons were cultured in a round Nunc culture dish (Thermo Fisher Scientific) from embryonic day 18 Charles River (CD) rats as described previously in Kumar et al. (2020). The EV pellets were harvested from the culture media of neurons treated with FGF2 (50 ng/ml) as per the guidelines provided by the International Society for Extracellular Vesicles (ISEV). The information on EV isolation method is submitted to EV TRACK (<sup>1</sup>EV-TRACK ID: EV200085). The isolated EV pellets were taken forward to perform MS analysis as described in Kumar et al. (2020). The MS results of differential EV proteomic signature were then subjected to further bioinformatics analysis.

### Validation of *Rab8b* and *Rab31* Abundance

The abundant expression of *Rab8b* and *Rab31* in EV pellets was confirmed via Western blot technique as described in Kumar et al. (2020). In brief, blots were prepared using Mini-Protean Gels from Bio-Rad and Tris-glycine-based buffer. Polyvinylidene difluoride (PVDF) membranes (Bio-Rad) were used to blot the proteins at 150 mA for 60–120 min while keeping them on ice. 5% skimmed milk in TBST buffer (tris–buffered saline containing 0.05% tween) was used as blocking solution for 1 h. After washing, membranes were incubated with primary antibodies [Rabbit polyclonal Rab8B (# PA5-67354) and Rabbit polyclonal Rab31 (# PA5-54064) (Thermo Fisher Scientific)] overnight at 4°C. The next day, membranes were washed and incubated with the respective secondary antibody. The blots were then developed by using Clarity Western blot ECL Substrate (Bio-Rad). LI-COR Odyssey Fc Imaging system was used to detect the chemiluminescence and analyzed by Image Studio

<sup>1</sup>evtrack.org

software (Licor). Western blot images were then used to calibrate the relative abundance of both candidate Rabs.

## PPiN, Pathways, and Cellular Component Enrichment Analysis

To construct a PPiN, we utilized the STRING v11 (accessed on 12/02/2020<sup>2</sup>) (Szklarczyk et al., 2019) online database. This resource assembles all known and predicted protein–protein interactions of organisms and consists of PPis based on the available experimental, text mining, and co-expression evidence. We retrieved the interactome (organism: *Rattus norvegicus*) of *Rab8b* and *Rab31* with the following criteria: (McCann et al., 2016) we considered an interaction as statistically significant at a >0.7 high confidence score (this cutoff is recommended by developers of STRING v11) (Braak et al., 2003b). To deduct all direct and indirect interactions of *Rab8b* and *Rab31*, we added the first shell of 100 and the second shell of 50 interactions. The *Rab8b* and *Rab31* interactome (RRi) map was visualized in Cytoscape v3.7.1 (Shannon et al., 2003). We calculated the average clustering coefficient and network heterogeneity using the Network Analyzer Cytoscape plugin (Shannon et al., 2003). The random network was generated based on the Erdos Renyi G ( $n,p$ ) model using the Network Randomizer Cytoscape plugin (Shannon et al., 2003). The pathway annotation of RRi was performed using METASCAPE (accessed on 12/02/2020<sup>3</sup>) (Zhou et al., 2019), which contains the biological process (BP) annotations and cellular components mined from gene ontology and pathways from KEGG. We considered functions and cellular components as statistically significant using a *P* value cutoff of <0.05.

## Cell Type and Brain Region Enrichment Analysis

To determine which proteins from the RRi are enriched in different brain cell types (microglia, oligodendrocytes, astrocytes, and neurons) and regions (optic nerve, brain stem, cerebellum, corpus callosum, OB, striatum, hippocampus, motor cortex, prefrontal cortex, and thalamus), we downloaded the lists of these proteins from the following site<sup>4</sup> (accessed on 14/02/2020) (Sharma et al., 2015). Prior to overlap analysis, we converted these mouse-specific gene symbols (we used gene symbols of proteome data) to rat ortholog gene symbols using the gProfiler online tool (<sup>5</sup>accessed on 14/02/2020) (Raudvere et al., 2019). We cross-referenced the rat gene symbols with RRi and assessed the enrichment of brain cell types and region proteins in RRi.

## ENS Analysis

To deduce the connection between the ENS and the RRi, we extracted the transcriptome signature from Roy-Carson et al. (2017). In this study, the authors generated gene expression profiles of a lineage-specific population of enteric progenitors

in zebrafish. We collected the up- and downregulated genes produced in Roy-Carson et al. (2017). We converted zebrafish gene symbols to rat orthologs (gene symbols) using the gProfiler online tool (see text footnote 5, accessed on 15/02/2020) (Raudvere et al., 2019). We mapped rat orthologs obtained from gProfiler onto RRi using Cytoscape v3.7.1 (Shannon et al., 2003).

## Mining of PD Proteins

To define if any Parkinson's disease (PD)-related proteins are enriched in RRis, we extracted PD proteome screens from publications (Dumitriu et al., 2016; Boerger et al., 2019; Lachen-Montes et al., 2019). Furthermore, we obtained PD-associated genes from the following resources: DisGeNET (<sup>6</sup>accessed on 16/02/2020) and Rat Genome Database (RGD) (<sup>7</sup>accessed on: 16/02/2020). We mined PD-associated genes from all the sources as mentioned above and translated their gene symbols to rat gene symbols using the gProfiler tool (accessed on 16/02/2020) (Raudvere et al., 2019). This list of rat gene symbols related to PD was finally intersected with RRi.

## Sequence Retrieval and Structural Modeling

To model the structures of *Rab8b*, *Rab3b*, and *Rab23* from the rat organism, we first retrieved protein sequences in fasta format from UniProt online database (<sup>8</sup>accessed on 22/07/2020). *Rab8b* (UniProt ID: P70550), *Rab3b* (UniProt ID: Q63941), and *Rab23* (UniProt ID: D3ZRM5) sequences were used as an input to SWISS-MODEL (Waterhouse et al., 2018) online software (<sup>9</sup>accessed on 22/07/2020) to model the three-dimensional (3D) protein structures. *Rab8b* was modeled based on template from Protein Data Bank (PDB) database (PDB ID: 6rlr.1.B); *Rab23* and *Rab3b* templates were also obtained from PDB (PDB IDs: 1z2a.1.A and 3dz8.1.A, respectively). The 3D models were selected for further analysis based on the Global Model Quality Estimation (GMQE) and Qualitative Model Energy Analysis (QMEAN) values. GMQE values range from 0 to 1; close to 1 represents reliability of the predicted 3D structure and QMEAN value <4.0 shows trustworthiness of structure. Then, atomic details such as correcting the side chains of structures were determined using the ModRefiner online tool (<sup>10</sup>accessed on 22/07/2020) (Xu and Zhang, 2011), and the Chiron online tool (<sup>11</sup>accessed on 22/07/2020) (Ramachandran et al., 2011) was used to remove steric clashes. ProSA-web online algorithm (Wiederstein and Sippl, 2007) (<sup>12</sup>accessed on 22/07/2020) was used to calculate the *z* score of the 3D structures to understand how well it is compared to experimental structures derived from X-ray or NMR.

<sup>6</sup>www.disgenet.org

<sup>7</sup>rgd.mcg.edu

<sup>8</sup>https://www.uniprot.org

<sup>9</sup>https://swissmodel.expasy.org

<sup>10</sup>https://zhanglab.ccmb.med.umich.edu/ModRefiner/

<sup>11</sup>https://dokhlab.med.psu.edu/chiron/login.php

<sup>12</sup>https://prosa.services.came.sbg.ac.at/prosa.php

<sup>2</sup>https://string-db.org

<sup>3</sup>https://metascape.org/

<sup>4</sup>www.mouseproteome.com

<sup>5</sup>https://biit.cs.ut.ee/gprofiler/orth

## Validation of Protein–Protein Interaction Using Docking

To predict the interaction between the Rab8b–Rab3b and Rab8b–Rab23 at the sequence level, we utilized protein sequences obtained from UniProt online database (see text footnote 8, accessed on 23/07/2020) and used the BIPSPI online tool (<sup>13</sup>accessed on 23/07/2020) (Sanchez-Garcia et al., 2019) to compute the interaction between the proteins. Then, we performed protein–protein (Rab8b–Rab3b) and (Rab8b–Rab23) docking to understand these interactions using a hybrid docking strategy with the HDOCK online server (<sup>14</sup>accessed on 23/07/2020) (Yan et al., 2017). Rab8b was used as receptor, and Rab3b and Rab23 were used as ligands. We used predicted binding site residues from sequence level analysis from the BIPSPI tool during docking analysis and default parameters. The docking scores between the protein–protein were computed using improved shape-based, pairwise scoring function in HDOCK.

## Statistical Evaluation and Data Visualization

The statistical evaluation and visualization in this study, if not stated otherwise, was executed using the R statistical environment v3.5.1<sup>15</sup>. Scatter plot, boxplot, and barplot were visualized using the ggplot2 R package. The PD-enriched protein heatmap was generated using Pheatmap R package. The percentage of *Rab8b* and *Rab31* direct and indirect interactions is visualized as a donut plot in Microsoft Excel. Statistical assessment of cell type and brain region protein overlap with RRI was done using Fisher's exact test, multiple comparisons were adjusted by the false discovery rate (FDR) ( $P < 0.05$ ) Benjamini–Hochberg (BH) method, and  $P$  values were converted to negative  $\log_{10}$ . 3D protein structure pictures were rendered in PyMOL software v2.3.0.

## RESULTS

### FGF2 Enriches *Rab8b* and *Rab31* in Neuronal EVs

Using at least three biological replicates, we recently assessed the global proteomic changes in EVs in response to treatment with FGF2 by performing a thorough MS analysis (Kumar et al., 2020). Out of 2258 differentially expressed proteins (DEPs), which were detected at least once in all samples, 705 were significantly expressed ( $FDR \leq 0.05$ ) and 441 proteins had a fold change of 1.5 or above (Kumar et al., 2020). Among the upregulated candidates, we found *Rab8b* and *Rab31* as prominent members of the Rab protein family with an increased abundance in EV pellets (**Supplementary Figure 1**). We cross-validated the proportional expression of these candidates along with EV biomarkers from their expression signals in MS data (**Supplementary Figure 2**).

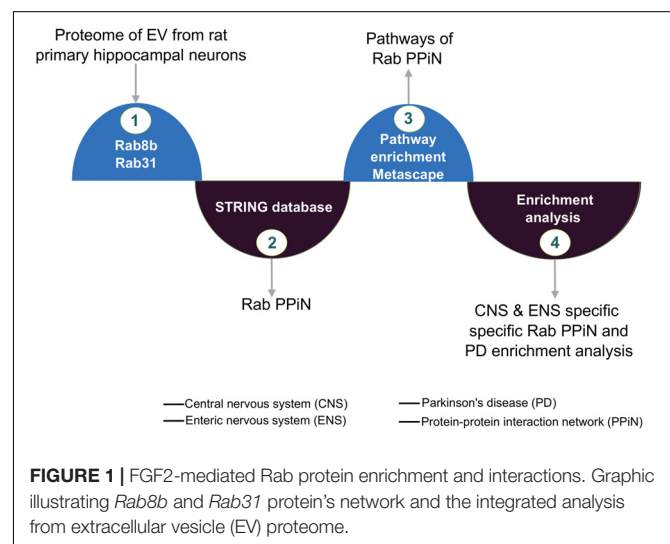
This enrichment was then considered for further analysis by subjecting it to a bioinformatic analysis (**Figure 1**).

### *Rab8b* Is a Key Effector in the *Rab8b*–*Rab31* Interactome

The EV proteome analysis revealed that FGF2 affects two specific Rab proteins, i.e., *Rab8b* and *Rab31*, where FGF2 increased the abundance of *Rab8b* up to 2-fold and that of *Rab31* up to  $\sim 1.5$ -fold (**Figure 2A**). In order to visualize the interactive network of these Rabs, we performed a PPI analysis to assess the full potential of FGF2-prompted *Rab8b* and *Rab31*. We extracted direct and indirect interaction partners through STRINGDB, yielding a *Rab8b*–*Rab31* interactome (RRI) (**Figure 2B**). At a very high confidence threshold cutoff ( $>0.7$ ), a total of 126 *Rab8b* and *Rab31* interactions were found. Among overlapping interacting proteins, a total number of 114 and 54 interactions were attributable to *Rab8b* and *Rab31*, respectively. This resulted in an individual interaction percentage of 90.48% for *Rab8b* and 42.86% for *Rab31*, making *Rab8b* the top contributor in the RRI (**Figure 2C**). Next, we examined the key topological properties such as average clustering coefficient (avg.cc) and network heterogeneity (nhet). We first computed the avg.cc in the RRI, compared it to a random network, and found significantly higher avg.cc in the RRI (**Figure 2D**). We observed higher nhet values for the RRI in contrast to a random network (**Figure 2E**). Taken together, our RRI analysis revealed *Rab8b* as a key effector. Furthermore, topological analysis showed that RRI is modular and very heterogeneous in nature, thus confirming that the interactome is controlled by central proteins.

### Neuronal Vesicle Release Sites Are Functional Epicenters of RRI

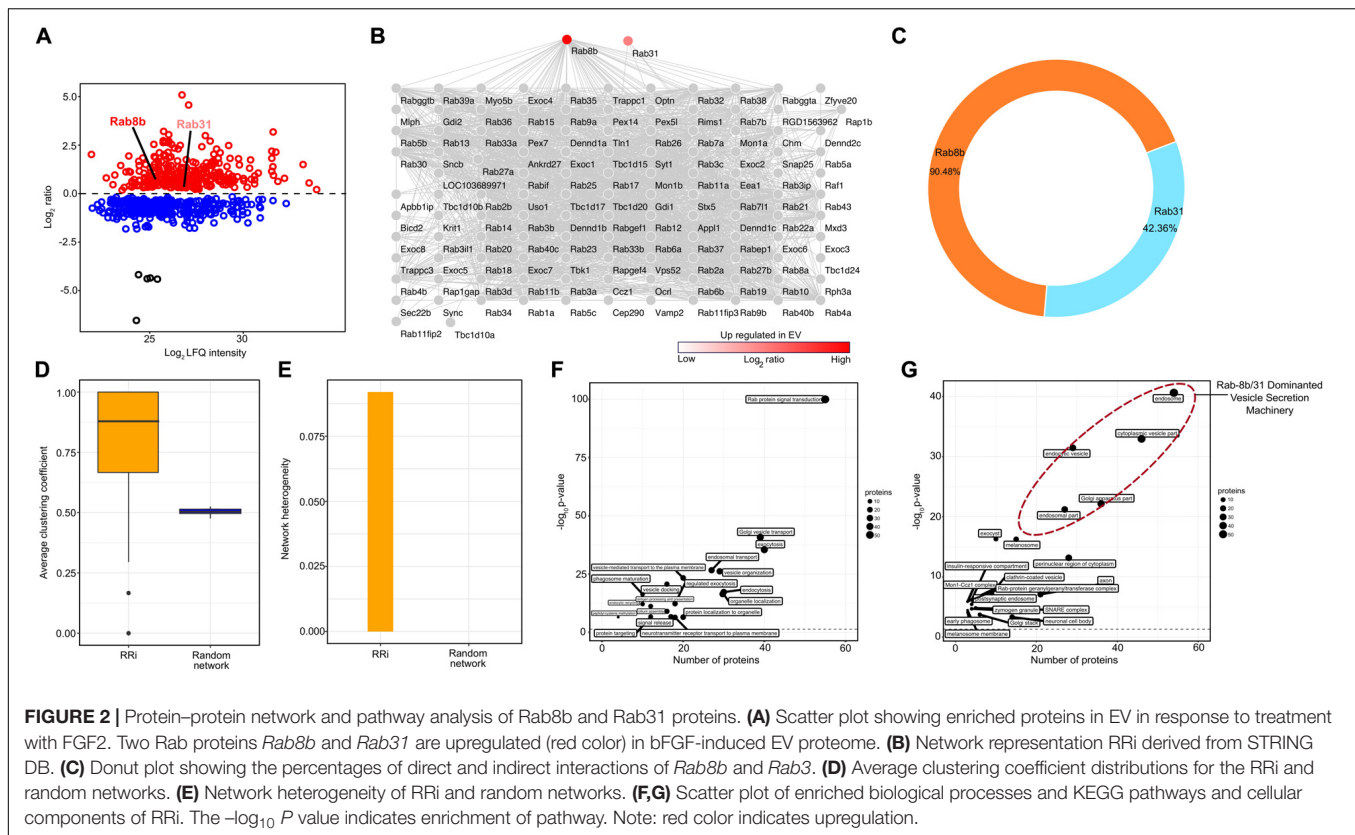
We obtained a functional readout of the RRI by subjecting the RRI dignitaries to a pathway enrichment analysis and found a number of vesicular secretion-related pathways enriched (**Figure 2F**). A higher significance and a high number of  $\sim 50$  candidates



<sup>13</sup><http://bipspi.cnb.csic.es/xgbPredApp/predictFormFromSeq/>

<sup>14</sup><http://hdock.phys.hust.edu.cn>

<sup>15</sup><https://www.r-project.org/>



enriching Rab protein signal transduction pathway was apparent from the participants of RRI. Pathways involved in vesicle secretion and membrane trafficking, e.g., Golgi vesicle transport, exocytosis, endocytosis, and protein localization to organelle, had a participation of  $\sim 40$  candidates, each scoring a very high significant  $P$  value cutoff of  $<0.05$ . Approximately 30 RRI members each exhibited a direct input to neuronal transport pathways like endosomal transport, vesicle-mediated transport to the plasma membrane, vesicle docking, protein localization to organelles, and neurotransmitter receptor transport to the plasma membrane. Other pathways such as phagosome maturation, endocytic recycling, signal release, and protein targeting were contributed by  $\sim 20$  nominees of each RRI and were significantly enriched. A detailed information on pathway participation by each candidate is included in **Supplementary Table 1**. The functional work stations of the RRI were attributed to the major neuronal compartments governing vesicle secretion (**Figure 2G**). Nearly 50 proteins were designated to an endosomal subcellular location,  $\sim 40$  to cytoplasmic vesicles, and  $\sim 30$  each to endocytic vesicles, the Golgi apparatus, and perinuclear regions of the cytoplasm including the major secretory machinery of neurons. Other subcellular locations involved in secretory processes such as post-synaptic endosomes, SNARE complexes, neuronal cell body, clathrin-coated vesicles, and early phagosome were recognized with a participatory candidature of  $\sim 20$  and 10 proteins each and were found above the significance cutoff. The individual candidature of proteins to subcellular locations is reported in **Supplementary Table 2**. Conclusively, from

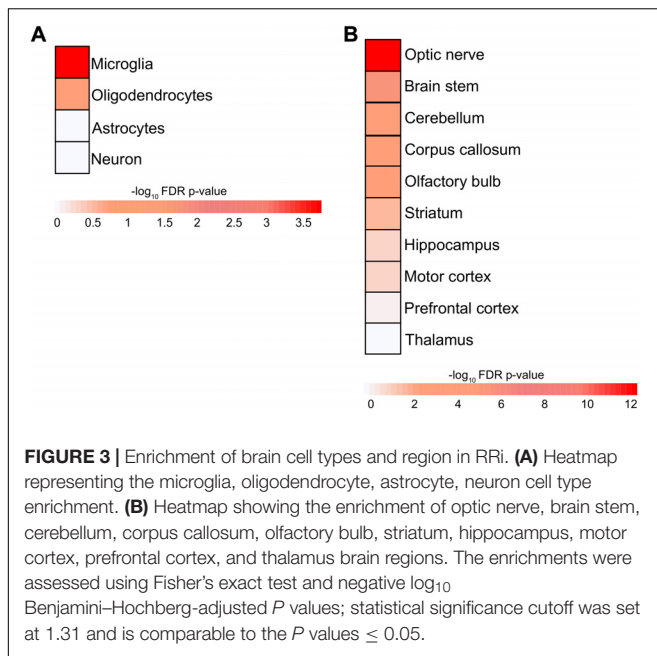
the subcellular location of RRI members, we concluded that FGF2-triggered enrichment of *Rab8b* and *Rab31* to EVs will likely influence early steps of EV biogenesis.

## RRI Has Its Implications to Other Native Brain Regions and Cells

Extracellular vesicles are capable of transmitting biomaterials from one cell to another and between different brain regions and are released by all CNS-resident cell types; therefore, an overlapping molecular machinery is expected. In order to investigate the potential interactions of RRIs in other brain cells, regions, and their peripheral extensions, we have mapped RRI proteins (RRIps) to indigenous proteomic signatures of respective neuronal components, cell types, and regions. This resulted in the highest enrichment ( $P < 0.05$ ) for glial cells, i.e., microglia and oligodendrocytes (**Figure 3A**). In line, our analysis depicted a greater overlap for the optic nerve, brain stem, cerebellum, corpus callosum, OB, and striatum native RRIps (**Figure 3B**). The results thus highlight the possible interaction of FGF2-stimulated EV-*Rab8b* and *Rab31* to the aforementioned respective sites.

## Annotation of Neuroglial Rabs Delineates the RRI Roles in Glial Action

To comprehend the neuroglial significance of RRI, we considered the hub Rab proteins reflected in significantly enriched glial components and developed a microglial specific Rab interactome (mSRi) (**Figure 4A**) and oligodendrocyte-specific



Rab interactome (oSRI) (Figure 4B). The mSRI had *Rab3il1*, *Rab27a*, *Rab32*, *Rab43*, and *Apbb1ip* as hub Rabs, whereas *Rab43* and *Rap1gap* were the hub proteins of oSRI. We individually subjected mSRI and oSRI to pathway enrichment analysis and found Rab protein signal transduction, endocytosis, and exocytosis as the top significantly enriched pathways. Interestingly, we observed an alternative enrichment of biological pathways for the mSRI and oSRI, with endocytosis as top hit of mSRI-Rabs and exocytosis of oSRI-Rabs allowing one to venture the possible global molecular interactions as a result of high FGF2 level in neurons.

### Pathological Relevance of mSRI and oSRI Along the Gut-Brain Axis Is Established by PD-ENS Rabs

As introduced earlier, the possibilities imposed by LB formation and its appearance in various CNS-ENS components and Rab interactions from mSRI and oSRI were identified in the background of their weight to the ENS, and their further ENS-PD participation was determined. We identified 71 ENS-PD-specific interactions, with 46 in mSRI and 25 in oSRI (Figures 4A,B). In mSRI, we identified *Rab6b*, *Rab3b*, *Rab21*, *Chm*, and *Rab23* as PD-Rabs, which had shown interactions with ENS-Rabs. *Rab6b* interacts with 10 other Rabs (*Rab2a*, *Rab3a*, *Rab3b*, *Rab3c*, *Rab3d*, *Rab33a*, *Rab15*, *Rab21*, *Rab23*, and *Rab27b*), which are present in ENS. Similarly, PD-Rabs *Rab3b* and *Chm* have 10 and 12 interactions with ENS-Rabs, respectively. PD-Rab *Rab23* and *Rab21* were found to be interacting with 3 and 11 other ENS-Rabs, respectively. Out of the total 25 PD-ENS oSRI Rab interactions, *Rab6b*, *Rab3b*, *Rab21*, and *Chm* had six interactions each; PD-Rab *Rap1b* had shown to be interacting with one *Rap1gap* ENS-Rab. All interaction nodes specific to PD-ENS Rabs were shown conjoined by colored lines between the nodes

(Figures 4A,B) and the individual functional contributions of PD-ENS interactions are presented in Supplementary Table 3. PD-Rabs *Rab2*, *Chm*, *Rab6b*, *Rab1b*, and *Rab3b* have shared candidature to both mSRI and oSRI, though *Rph3a*, *Rab23*, and *Tln1* were microglia-specific PD-associated Rabs (Figure 4C).

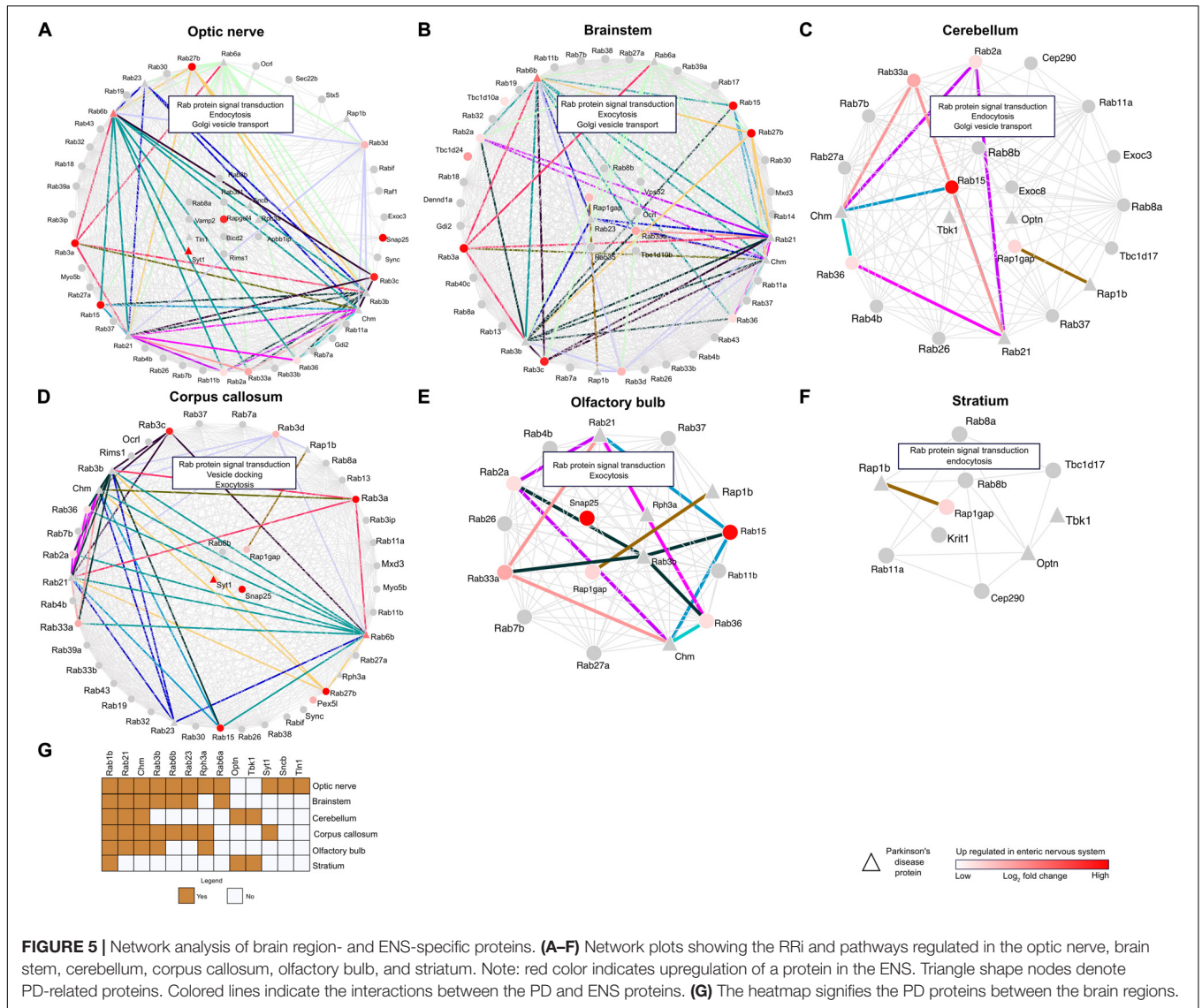
### Alternative Functional Enrichment by Brain-Region-Specific Rabs Sketches the FGF2-Induced EV-Mediated Pathology Offshoot

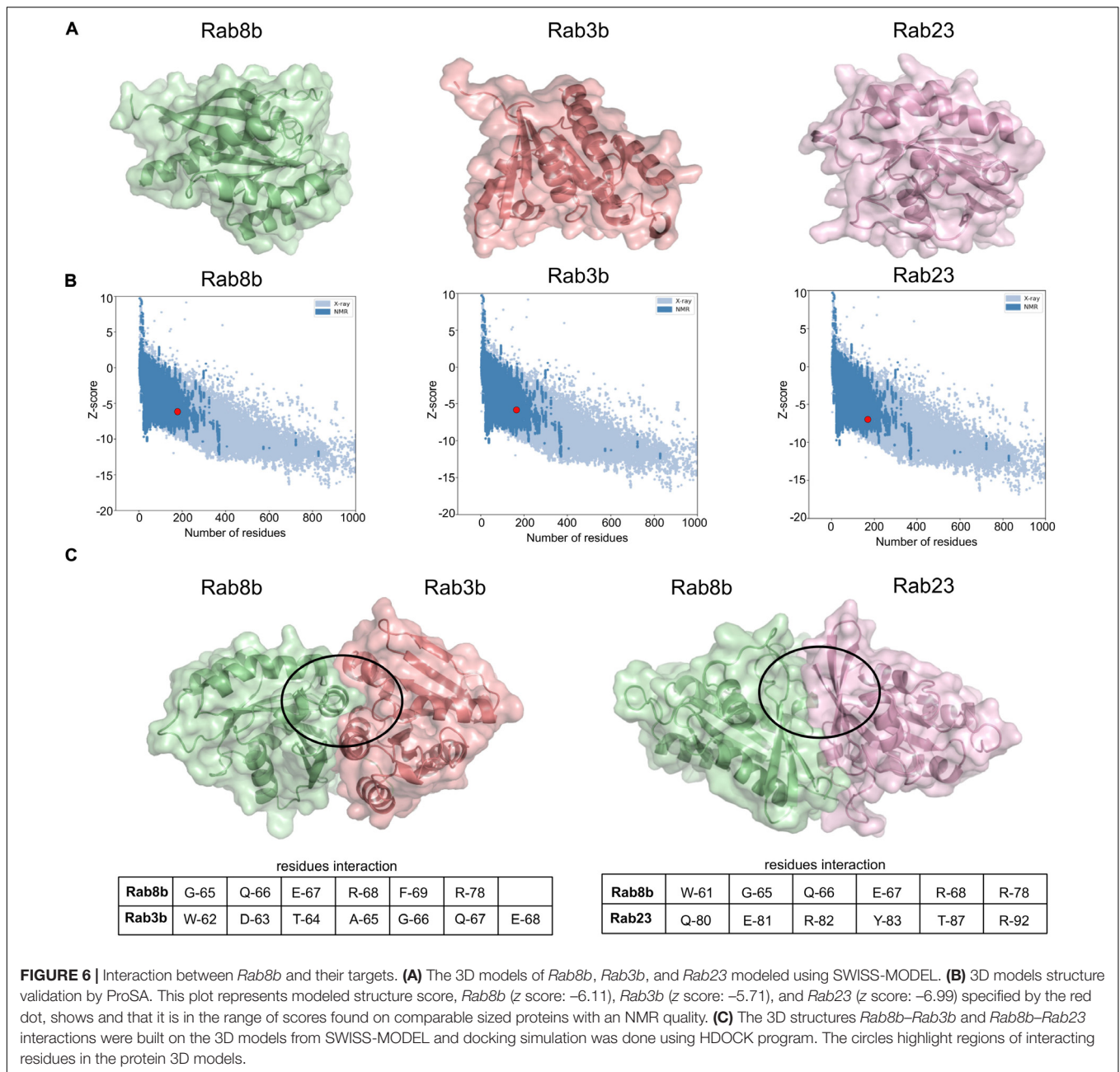
The RRIps were mapped to CNS-specific proteome signatures, and significantly enriched regions were considered for further analyses of region-specific Rab interactions. Brain-region-specific sub-RRIs for each significantly enriched region were developed. This approach resulted in optic-nerve-specific Rab infraction (oSRI) (Figure 5A), brain-stem-specific Rab infraction (bsSRI) (Figure 5B), cerebellum-specific Rab infraction (ceSRI) (Figure 5C), corpus-callosum-specific Rab infraction (ccSRI) (Figure 5D), olfactory-bulb-specific Rab infraction (obSRI) (Figure 5E), and striatum-specific Rab infraction (stSRI) (Figure 5F) subnets. The functional hubs of these interactions in sub-RRIs were detected, and these hub Rab proteins would therefore represent the key Rab molecules in the respective anatomical brain segment under the potential influence of FGF2 and may therefore govern the CNS-specific Rab infractions. For onSRI, *Rab8b*, *Rab8a*, *Rab3il1*, *Sncb*, *Rph3a*, *Vamp2*, *Rapgef4*, *Tln1*, *Bicd2*, *Apbb1ip*, *Rims1*, and *Syt1* were the hub proteins along with Rab signal transduction, endocytosis, and Golgi vesicle transport as the key enriched biological pathways. In bsSRI, we found *Rab8b*, *Vps52*, *Rap1gap*, *Ocrl*, *Rab23*, *Rab33a*, *Rab35*, and *Tbcl10b* as key hubs contributing to biological pathway Rab signal transduction, exocytosis, and Golgi vesicle transport. The ceSRI hubs were *Rab8b*, *Exoc8*, *Optn*, *Rab15*, and *Tbk1* enriching Rab signal transduction, endocytosis, and Golgi vesicle transport as top functional pathways via their interactions. *Rab8b*, *Rap1gap*, *Syt1*, and *Snap25* were the hub molecules in ccSRI showing top enrichment of Rab signal transduction, exocytosis, and vesicle docking pathways. For obSRI, key governing molecules were *Snap25*, *Rph3A*, *Rap1gap*, and *Rab3b* sharing Rab signal transduction and exocytosis as top enriched pathways altogether from their interactions. *Rab8b* and *Rap1gap* were the central molecules for stSRI and enriched Rab signal transduction and endocytosis as main pathways. The enrichment of Rab signal transduction as the key pathway among all sub-RRIs is obvious from the key Rab interactions, also highlighting the alternative enrichment of exocytosis and endocytosis as core functional enrichment to various brain regions.

### Brain-Region-Specific PD-ENS Rabs Settle FGF2-Induced Rab Enrichment Along the Gut-Brain Axis

In total, 181 ENS-PD-specific interactions were identified among CNS-specific Rab infractions (CNS-RRi) in rat orthologs, out of which 46 were found in onSRI, 58 in bsSRI, 10 in ceSRI, 48 in ccSRI, 18 in obSRI, and 1 in stSRI (Figures 5A-F).







*Rab8b* as a key regulator of the RRI (Figure 2C). Topological analysis demonstrated that RRI is modular and consists of highly connected proteins (Figures 2D,E). Earlier studies confirmed that *Rab8b* is an interacting partner of Otoferlin, which is a protein associated to hearing loss (Heidrych et al., 2008). Several genetic alterations to Otoferlin are found to be associated to the pathogenicity of hearing-related disorders (Varga et al., 2006), and PD patients are found prone to hearing loss or having difficulties in processing auditory inputs (Folmer et al., 2017). Therefore, *Rab8b* enrichment in EVs stimulated by high FGF2 levels (reported for the first time in our study) and its interactions supports a novel possibility of explaining molecular

basis of non-motor symptoms like hearing loss in PD pathology (Vitale et al., 2012). Furthermore, hearing loss is associated to dementia as reported in Lin et al. (2011), and the relevance of the hippocampus in DLB is known (Liu et al., 2019). Autopsies of PD and DLB patients suggests a spreading of pathology among the brain regions, a role of hippocampal  $\alpha$ -Syn in the loss of cognitive functions, and additional non-motor symptoms across the parkinsonian pathology spectrum (Adamowicz et al., 2017). These results thus highlight the overall significance of our study on hippocampal neurons. The functional enrichment analysis and subcellular segregation of RRI members support the idea of FGF2 influencing EV biogenesis (Figures 2F,G). From

earlier studies, it has been reported that *Rab8b* promotes the caveolin-mediated endocytosis of certain receptors during early endosome formation that subsequently fuse with multi-vesicular bodies (MVBs) and therefore facilitates the EV biogenesis (Demir et al., 2013). Moreover, *Rab31* has been shown to have a role in the endocytic trafficking of growth factor receptors and regulation of the early endosome antigen 1 (EEA1), a trafficking complex formation, which is a pre-step implicated in EV biogenesis (Chua et al., 2014). These early involvements in vesicle secretion cycle thus establish the roles of *Rab8b* and *Rab31* in the cargo-dependent fate of EVs, which is also counter supported by the fact that they are enriched to EVs specifically after FGF2 treatment.

The relevance of EV-associated Rab enrichment for PD pathology was further assessed via the global effect of RRI interactions, obtained from mapping RRI members to native proteomic orthologs, and we identified significantly enriched Rabs specific to CNS cells and anatomical regions (Figures 3A,B). The significant enrichment of glial cells in our mapping analysis may be due to the high availability of publicly accessible data, which are often derived from glial cells in the context of EVs. In addition, the fact that a high number of investigations focused mainly on secretory pathways may limit the conclusions of this work. Yet, the identification of an alternative functional enrichment by mSRi and oSRi Rabs supports previewing a Rab-mediated CNS homeostatic regulation sieged by high FGF2 levels and is likely primed via EV secretion (Figures 4A,B). The specific enrichment of exocytosis from oSRi and endocytosis by mSRi as key pathways supports a cross-talk concomitant to glial cells. The parallel appearance of LBs in glial cells further validates such cross-talk (Braak et al., 2007). It has been shown that inclusion burden in glial cells is directly proportional to the loss of SNc neurons (Wakabayashi et al., 2000). The appearance of *Apbb1ip* as one of the hub proteins in the Rab interactome and the presence of microglia-specific *Tln* in mSRi support the possibility of a FGF2-enhanced LB formation (Figures 4A,C). It has been reported that *Apbb1ip* directly interacts with *Tln* and is further required to activate integrins, a family of adhesion molecules (Lee et al., 2009). In leukocytes, it has been shown that a lack of *Apbb1ip* results in adhesion deficiency of leukocytes (Klapproth et al., 2015). Such adhesion deficit insinuations allow us to deduce a hypothetical model of LB formation by means of protein misfolding tethered through “protein-stickiness” and subsequently accompanied by other associated interactions of PD-related Rabs at high FGF2 levels. Furthermore, the hippocampal expression of *Apbb1ip* makes it a favorable candidate to discern the molecular pathophysiology of dementia in PD patients (Moradifard et al., 2018).

It became clear now that dopamine (DA) depletion does not correlate significantly with non-motor symptoms in PD patients and that they retain high growth factor levels with a distinct inflammatory profile (Brockmann et al., 2017; Park et al., 2019). Alongside the consecutive appearance of LBs, it is therefore important to consider cells and brain regions beyond SNc-DA neurons and examine the respective pathology correlates. Our mapping analysis allowed us to identify significantly enriched brain regions for RRI members and to develop a brain-region-specific Rab interactome (Figures 5A–F). Furthermore,

alterations of the endocytosis/exocytosis pathway enrichment in different brain regions may explain how EVs transfer malicious proteins and ultimately enhance the pathology spread with Rab mediation. In line with exocytosis as the main pathway enriched in the brain stem, OB and corpus callosum could provide a preliminary map of “release centers,” whereas the alternative enrichment of endocytosis as the main pathway in other brain regions could act as “receiving centers.”

The appearance of *Ocr1* as a hub molecule in brain-stem-specific bsSRi (Figure 5B) is interesting, since the brain stem may act as an input point in a pathology progression interceded from the ENS to CNS (Braak et al., 2003a; Abbott et al., 2007). Therefore, we have resolved the ENS-allied Rabs in all the interactomes, which could possibly delineate the Rab-governed pathology along the gut–brain axis (Figures 4, 5). This could further be affirmed by the fact that *Ocr1* is involved in the regulation of early endosomes in a Rab-dependent manner and shares a binding site with *App11*, another endocytic protein (Schenck et al., 2008; Swan et al., 2010). The fate of such interactions could therefore further mediate the transmission of LB-associated content in EVs and hence establish the brain stem as a “relay center.” This gains further support by the finding that bsSRi candidates specifically designate exocytosis as the top outcome in our functional pathway enrichment analysis. The association of *Ocr1* to other disorders like Lowe syndrome and Dent disease signifies the role of these interactions beyond PD pathology and may serve as a merging point for many symptoms across the parkinsonian symptom spectrum (De Matteis et al., 2017). The presence of *Rab3b* among the top coinciding PD-Rabs (Figure 5G) may explain a possible epigenetic association as a consequence of its age-related methylation (Li et al., 2019). Furthermore, our docking analysis validates *Rab3b* and *Rab23* as much stronger and more stable interaction partners of *Rab8b* with lowest docking energies that are proportional to the strength of interaction (Figure 6C).

We conversed to the use of rat orthologues in our study to build on FGF2-facilitated *Rab8b* and *Rab31* enrichment to EVs in a more concrete manner by outlining the sub-interactomes only among the close-knitted interactions, though it had restricted us to a limited number of interactions. A further wet-lab validation in brain tissue would directly suffice the specificity and relevance of these interactions. Collectively, this study generates support for the cargo-dependent fate of EVs, because FGF2 triggers enrichment of specific Rabs to EVs and further highlights a Rab-mediated foreground for LB formation and intercellular trafficking defects linked to PD symptoms. Our study supports the idea of allied molecular precursors that could possibly supplement a physiologically favorable state during the onset of PD pathology.

## DATA AVAILABILITY STATEMENT

The EV proteome dataset analyzed in this study can be found in the ProteomeXchange Consortium via the PRIDE partner repository under accession number: PXD014401.

## ETHICS STATEMENT

The animal study was reviewed and approved by Local authorities and the animal welfare committee of the Ludwig Maximilian University of Munich, Germany.

## AUTHOR CONTRIBUTIONS

RK conceived the project. RK, SD, and SM conducted the research. RK, SD, and TK wrote the manuscript. TK, KB, and GH supervised the project. All authors have read and agreed to the published version of the manuscript.

## FUNDING

This study was supported by the Deutsche Forschungsgemeinschaft (German Research Foundation) (DFG, HO2402/18-1 MSA omics) within the framework of the Munich Cluster for Systems Neurology (EXC 2145 SyNergy) and by the Parkinson Fonds Deutschland, the Hilde-Ulrichs-Stiftung, the Friede

Springer Stiftung, and the Lüneburg-Heritage for Parkinson's disease research. GH was funded by the German Federal Ministry of Education and Research (BMBF, 01KU1403A EpiPD; 01EK1605A HitTau), the ParkinsonFonds Germany (Hypothesis-free compound screen, alpha-Synuclein fragments in PD), and the VolkswagenStiftung/Lower Saxony Ministry for Science/Petermax-Müller Foundation (Etiology and Therapy of Synucleinopathies and Tauopathies).

## ACKNOWLEDGMENTS

RK would like to thank the organizers of NETTAB/BBCC 2019 conference for considering our preliminary results for the conference which served as a precursor of this work.

## SUPPLEMENTARY MATERIAL

The Supplementary Material for this article can be found online at: <https://www.frontiersin.org/articles/10.3389/fgene.2020.572058/full#supplementary-material>

## REFERENCES

- Abbott, R. D., Ross, G. W., Petrovitch, H., Tanner, C. M., Davis, D. G., Masaki, K. H., et al. (2007). Bowel movement frequency in late-life and incidental Lewy bodies. *Mov. Disord.* 22, 1581–1586. doi: 10.1002/mds.21560
- Adamowicz, D. H., Roy, S., Salmon, D. P., Galasko, D. R., Hansen, L. A., Masliah, E., et al. (2017). Hippocampal  $\alpha$ -Synuclein in dementia with lewy bodies contributes to memory impairment and is consistent with spread of pathology. *J. Neurosci.* 37, 1675–1684. doi: 10.1523/jneurosci.3047-16.2016
- Araujo, D. M., Lapchak, P. A., and Hefti, F. (1993). Effects of chronic basic fibroblast growth factor administration to rats with partial fimbrial transections on presynaptic cholinergic parameters and muscarinic receptors in the hippocampus: comparison with nerve growth factor. *J. Neurochem.* 61, 899–910. doi: 10.1111/j.1471-4159.1993.tb03601.x
- Boerger, M., Funke, S., Leha, A., Roser, A. E., Wuestemann, A. K., Maass, F., et al. (2019). Proteomic analysis of tear fluid reveals disease-specific patterns in patients with Parkinson's disease - A pilot study. *Parkins. Relat. Disord.* 63, 3–9. doi: 10.1016/j.parkrel.2019.03.001
- Braak, H., and Del Tredici, K. (2017). Neuropathological staging of brain pathology in sporadic parkinson's disease: separating the wheat from the chaff. *J. Parkinson Dis.* 7, S71–S85.
- Braak, H., Rüb, U., Gai, W. P., and Del Tredici, K. (2003a). Idiopathic Parkinson's disease: possible routes by which vulnerable neuronal types may be subject to neuroinvasion by an unknown pathogen. *J. Neural Trans.* 110, 517–536. doi: 10.1007/s00702-002-0808-2
- Braak, H., Tredici, K. D., Rüb, U., de Vos, R. A. I., Jansen Steur, E. N. H., and Braak, E. (2003b). Staging of brain pathology related to sporadic Parkinson's disease. *Neurobiol. Aging* 24, 197–211. doi: 10.1016/s0197-4580(02)00065-9
- Braak, H., Sastre, M., and Del Tredici, K. (2007). Development of  $\alpha$ -synuclein immunoreactive astrocytes in the forebrain parallels stages of intraneuronal pathology in sporadic Parkinson's disease. *Acta Neuropathol.* 114, 231–241. doi: 10.1007/s00401-007-0244-3
- Breda, C., Nugent, M. L., Estranero, J. G., Kyriacou, C. P., Outeiro, T. F., Steinert, J. R., et al. (2015). Rab11 modulates alpha-synuclein-mediated defects in synaptic transmission and behaviour. *Hum. Mol. Genet.* 24, 1077–1091. doi: 10.1093/hmg/ddu521
- Brockmann, K., Schulte, C., Schneiderhan-Marra, N., Apel, A., Pont-Sunyer, C., Vilas, D., et al. (2017). Inflammatory profile discriminates clinical subtypes in LRRK2-associated Parkinson's disease. *Eur. J. Neurol.* 24:427.e6.
- Cavaliere, F., Cerf, L., Dehay, B., Ramos-Gonzalez, P., De Giorgi, F., Bourdenx, M., et al. (2017). In vitro alpha-synuclein neurotoxicity and spreading among neurons and astrocytes using Lewy body extracts from Parkinson disease brains. *Neurobiol. Dis.* 103, 101–112. doi: 10.1016/j.nbd.2017.04.011
- Chang, C., Lang, H., Geng, N., Wang, J., Li, N., and Wang, X. (2013). Exosomes of BV-2 cells induced by alpha-synuclein: important mediator of neurodegeneration in PD. *Neurosci. Lett.* 548, 190–195. doi: 10.1016/j.neulet.2013.06.009
- Chua, C. E. L., Goh, E. L. K., and Tang, B. L. (2014). Rab31 is expressed in neural progenitor cells and plays a role in their differentiation. *FEBS Lett.* 588, 3186–3194. doi: 10.1016/j.febslet.2014.06.060
- Cooper, A. A., Gitler, A. D., Cashikar, A., Haynes, C. M., Hill, K. J., Bhullar, B., et al. (2006).  $\alpha$ -Synuclein Blocks ER-Golgi traffic and rab1 rescues neuron loss in Parkinson models. *Science* 313:324. doi: 10.1126/science.1129462
- De Matteis, M. A., Staiano, L., Emma, F., and Devuyt, O. (2017). The 5-phosphatase OCRL in Lowe syndrome and Dent disease 2. *Nat. Rev. Nephrol.* 13, 455–470. doi: 10.1038/nrneph.2017.83
- Demir, K., Kirsch, N., Beretta Carlo, A., Erdmann, G., Ingelfinger, D., Moro, E., et al. (2013). RAB8B is required for activity and caveolar endocytosis of LRP6. *Cell Rep.* 4, 1224–1234. doi: 10.1016/j.celrep.2013.08.008
- Dettmer, U., Ramalingam, N., von Saucken, V. E., Kim, T. E., Newman, A. J., Terry-Kantor, E., et al. (2017). Loss of native alpha-synuclein multimerization by strategically mutating its amphipathic helix causes abnormal vesicle interactions in neuronal cells. *Hum. Mol. Genet.* 26, 3466–3481. doi: 10.1093/hmg/ddx227
- Dumitriu, A., Golji, J., Labadorf, A. T., Gao, B., Beach, T. G., Myers, R. H., et al. (2016). Integrative analyses of proteomics and RNA transcriptomics implicate mitochondrial processes, protein folding pathways and GWAS loci in Parkinson disease. *BMC Med. Genom.* 9:5. doi: 10.1186/s12920-016-0164-y
- Folmer, R. L., Vachhani, J. J., Theodoroff, S. M., Ellinger, R., and Riggins, A. (2017). Auditory processing abilities of Parkinson's disease patients. *Biomed. Res. Int.* 2017:2618587.
- Grey, M., Dunning, C. J., Gaspar, R., Grey, C., Brundin, P., Sparr, E., et al. (2015). Acceleration of alpha-synuclein aggregation by exosomes. *J. Biol. Chem.* 290, 2969–2982. doi: 10.1074/jbc.m114.585703
- Hall, H., Reyes, S., Landeck, N., Bye, C., Leanza, G., Double, K., et al. (2014). Hippocampal Lewy pathology and cholinergic dysfunction are associated with

- dementia in Parkinson's disease. *Brain* 137(Pt 9), 2493–2508. doi: 10.1093/brain/awu193
- Heidrych, P., Zimmermann, U., Breß, A., Pusch, C. M., Ruth, P., Pfister, M., et al. (2008). Rab8b GTPase, a protein transport regulator, is an interacting partner of otoferlin, defective in a human autosomal recessive deafness form. *Hum. Mol. Genet.* 17, 3814–3821. doi: 10.1093/hmg/ddn279
- Holmqvist, S., Chutna, O., Bousset, L., Aldrin-Kirk, P., Li, W., Bjorklund, T., et al. (2014). Direct evidence of Parkinson pathology spread from the gastrointestinal tract to the brain in rats. *Acta Neuropathol.* 128, 805–820. doi: 10.1007/s00401-014-1343-6
- Hunn, B. H., Cragg, S. J., Bolam, J. P., Spillantini, M. G., and Wade-Martins, R. (2015). Impaired intracellular trafficking defines early Parkinson's disease. *Trends Neurosci.* 38, 178–188. doi: 10.1016/j.tins.2014.12.009
- Jones, D. R., Delenclos, M., Baine, A. T., DeTure, M., Murray, M. E., Dickson, D. W., et al. (2015). Transmission of soluble and insoluble alpha-synuclein to mice. *J. Neuropathol. Exper. Neurol.* 74, 1158–1169. doi: 10.1093/jnen/74.12.1158
- Kiral, F. R., Kohrs, F. E., Jin, E. J., and Hiesinger, P. R. (2018). Rab GTPases and membrane trafficking in neurodegeneration. *Curr. Biol.* 28, R471–R486.
- Klapproth, S., Sperandio, M., Pinheiro, E. M., Prünster, M., Soehnlein, O., Gertler, F. B., et al. (2015). Loss of the Rap1 effector RIAM results in leukocyte adhesion deficiency due to impaired  $\beta 2$  integrin function in mice. *Blood* 126, 2704–2712. doi: 10.1182/blood-2015-05-647453
- Kumar, R., Tang, Q., Müller, S. A., Gao, P., Mahlstedt, D., Zampagni, S., et al. (2020). Fibroblast Growth Factor 2-mediated regulation of neuronal exosome release depends on VAMP3/cellubrevin in hippocampal neurons. *Adv. Sci.* 7:1902372. doi: 10.1002/adv.201902372
- Lachen-Montes, M., Gonzalez-Morales, A., Iloro, I., Elortza, F., Ferrer, I., Gveric, D., et al. (2019). Unveiling the olfactory proteostatic disarrangement in Parkinson's disease by proteome-wide profiling. *Neurobiol. Aging* 73, 123–134. doi: 10.1016/j.neurobiolaging.2018.09.018
- Le, N. Q., Ho, Q. T., and Ou, Y. Y. (2018). Classifying the molecular functions of Rab GTPases in membrane trafficking using deep convolutional neural networks. *Analyt. Biochem.* 555, 33–41. doi: 10.1016/j.ab.2018.06.011
- Le, N. Q. K., Ho, Q. T., and Ou, Y. Y. (2019). Using two-dimensional convolutional neural networks for identifying GTP binding sites in Rab proteins. *J. Bioinform. Comput. Biol.* 17:1950005. doi: 10.1142/s0219720019500057
- Lee, H.-S., Lim, C. J., Puzon-McLaughlin, W., Shattil, S. J., and Ginsberg, M. H. (2009). RIAM activates integrins by linking Talin to Ras GTPase membrane-targeting sequences. *J. Biol. Chem.* 284, 5119–5127. doi: 10.1074/jbc.m807117200
- Li, G., Petkova, T. D., Laritsky, E., Kessler, N., Baker, M. S., Zhu, S., et al. (2019). Early postnatal overnutrition accelerates aging-associated epigenetic drift in pancreatic islets. *Environ. Epigenet.* 5:dvz015.
- Li, J. Y., Englund, E., Holton, J. L., Soulet, D., Hagell, P., Lees, A. J., et al. (2008). Lewy bodies in grafted neurons in subjects with Parkinson's disease suggest host-to-graft disease propagation. *Nat. Med.* 14, 501–503. doi: 10.1038/nm1746
- Lin, F. R., Metter, E. J., O'Brien, R. J., Resnick, S. M., Zonderman, A. B., and Ferrucci, L. (2011). Hearing loss and incident dementia. *Archiv. Neurol.* 68, 214–220.
- Liu, A. K. L., Chau, T. W., Lim, E. J., Ahmed, I., Chang, R. C.-C., Kalaitzakis, M. E., et al. (2019). Hippocampal CA2 Lewy pathology is associated with cholinergic degeneration in Parkinson's disease with cognitive decline. *Acta Neuropathol. Commun.* 7:61.
- McCann, H., Cartwright, H., and Halliday, G. M. (2016). Neuropathology of alpha-synuclein propagation and braak hypothesis. *Mov. Disord.* 31, 152–160. doi: 10.1002/mds.26421
- Mignogna, M. L., and D'Adamo, P. (2018). Critical importance of RAB proteins for synaptic function. *Small GTPases* 9, 145–157. doi: 10.1080/21541248.2016.1277001
- Moradifard, S., Hoseinbeyki, M., Ganji, S. M., and Minucheher, Z. (2018). Analysis of microRNA and Gene expression profiles in Alzheimer's disease: a meta-analysis approach. *Sci. Rep.* 8:4767.
- Ng, E. L., and Tang, B. L. (2008). Rab GTPases and their roles in brain neurons and glia. *Brain Res. Rev.* 58, 236–246. doi: 10.1016/j.brainresrev.2008.04.006
- Ngolab, J., Trinh, I., Rockenstein, E., Mante, M., Florio, J., Trejo, M., et al. (2017). Brain-derived exosomes from dementia with Lewy bodies propagate  $\alpha$ -synuclein pathology. *Acta Neuropathol. Commun.* 5:46.
- Park, S. B., Kwon, K.-Y., Lee, J.-Y., Im, K., Sunwoo, J.-S., Lee, K. B., et al. (2019). Lack of association between dopamine transporter loss and non-motor symptoms in patients with Parkinson's disease: a detailed PET analysis of 12 striatal subregions. *Neurol. Sci.* 40, 311–317. doi: 10.1007/s10072-018-3632-7
- Ramachandran, S., Kota, P., Ding, F., and Dokholyan, N. V. (2011). Automated minimization of steric clashes in protein structures. *Proteins* 79, 261–270. doi: 10.1002/prot.22879
- Raudvere, U., Kolberg, L., Kuzmin, I., Arak, T., Adler, P., Peterson, H., et al. (2019). g:Profiler: a web server for functional enrichment analysis and conversions of gene lists (2019 update). *Nucleic Acids Res.* 47, W191–W198.
- Roy-Carson, S., Natukunda, K., Chou, H. C., Pal, N., Farris, C., Schneider, S. Q., et al. (2017). Defining the transcriptomic landscape of the developing enteric nervous system and its cellular environment. *BMC Genom.* 18:290. doi: 10.1186/s12864-017-3653-2
- Sanchez-Ferro, A., Rabano, A., Catalan, M. J., Rodriguez-Valcarcel, F. C., Fernandez Diez, S., Herreros-Rodriguez, J., et al. (2015). In vivo gastric detection of alpha-synuclein inclusions in Parkinson's disease. *Mov. Disord.* 30, 517–524. doi: 10.1002/mds.25988
- Sanchez-Garcia, R., Sorzano, C. O. S., Carazo, J. M., and Segura, J. (2019). BIPSPi: a method for the prediction of partner-specific protein-protein interfaces. *Bioinformatics* 35, 470–477.
- Schenck, A., Goto-Silva, L., Collinet, C., Rhinn, M., Giner, A., Habermann, B., et al. (2008). The endosomal protein Appl1 mediates Akt substrate specificity and cell survival in vertebrate development. *Cell* 133, 486–497. doi: 10.1016/j.cell.2008.02.044
- Shannon, P., Markiel, A., Ozier, O., Baliga, N. S., Wang, J. T., Ramage, D., et al. (2003). Cytoscape: a software environment for integrated models of biomolecular interaction networks. *Genome Res.* 13, 2498–2504. doi: 10.1101/gr.1239303
- Sharma, K., Schmitt, S., Bergner, C. G., Tyanova, S., Kannaiyan, N., Manrique-Hoyos, N., et al. (2015). Cell type- and brain region-resolved mouse brain proteome. *Nat. Neurosci.* 18, 1819–1831. doi: 10.1038/nn.4160
- Shikanai, M., Yuzaki, M., and Kawachi, T. (2018). Rab family small GTPases-mediated regulation of intracellular logistics in neural development. *Histol. Histopathol.* 33, 765–771.
- Shults, C. W. (2006). Lewy bodies. *Proc. Natl. Acad. Sci. U.S.A.* 103:1661.
- Stuendl, A., Kunadt, M., Kruse, N., Bartels, C., Moebius, W., Danzer, K. M., et al. (2016). Induction of alpha-synuclein aggregate formation by CSF exosomes from patients with Parkinson's disease and dementia with Lewy bodies. *Brain* 139(Pt 2), 481–494. doi: 10.1093/brain/awv346
- Swan, L. E., Tomasini, L., Pirruccello, M., Lunardi, J., and De Camilli, P. (2010). Two closely related endocytic proteins that share a common OCRL-binding motif with APPL1. *Proc. Natl. Acad. Sci. U.S.A.* 107:3511. doi: 10.1073/pnas.0914658107
- Szkarczyk, D., Gable, A. L., Lyon, D., Junge, A., Wyder, S., Huerta-Cepas, J., et al. (2019). STRING v11: protein-protein association networks with increased coverage, supporting functional discovery in genome-wide experimental datasets. *Nucleic Acids Res.* 47, D607–D613.
- Varga, R., Avenarius, M. R., Kelley, P. M., Keats, B. J., Berlin, C. I., Hood, L. J., et al. (2006). OTOF mutations revealed by genetic analysis of hearing loss families including a potential temperature sensitive auditory neuropathy allele. *J. Med. Genet.* 43, 576–581. doi: 10.1136/jmg.2005.038612
- Villarreal-Campos, D., Bronfman, F. C., and Gonzalez-Billault, C. (2016). Rab GTPase signaling in neurite outgrowth and axon specification. *Cytoskeleton* 73, 498–507. doi: 10.1002/cm.21303
- Vitale, C., Marcelli, V., Allocca, R., Santangelo, G., Riccardi, P., Erro, R., et al. (2012). Hearing impairment in Parkinson's disease: expanding the nonmotor phenotype. *Mov. Disord.* 27, 1530–1535. doi: 10.1002/mds.25149
- Volpicelli-Daley, L. A., Gamble, K. L., Schultheiss, C. E., Riddle, D. M., West, A. B., and Lee, V. M. (2014). Formation of alpha-synuclein Lewy neurite-like aggregates in axons impedes the transport of distinct endosomes. *Mol. Biol. Cell* 25, 4010–4023. doi: 10.1091/mbc.e14-02-0741
- Wakabayashi, K., Hayashi, S., Yoshimoto, M., Kudo, H., and Takahashi, H. (2000). NACP/ $\alpha$ -synuclein-positive filamentous inclusions in astrocytes and oligodendrocytes of Parkinson's disease brains. *Acta Neuropathol.* 99, 14–20. doi: 10.1007/pl00007400
- Waterhouse, A., Bertoni, M., Bienert, S., Studer, G., Tauriello, G., Gumienny, R., et al. (2018). SWISS-MODEL: homology modelling of protein structures and complexes. *Nucleic Acids Res.* 46, W296–W303.

- Wiederstein, M., and Sippl, M. J. (2007). ProSA-web: interactive web service for the recognition of errors in three-dimensional structures of proteins. *Nucleic Acids Res.* 35, W407–W410.
- Xu, D., and Zhang, Y. (2011). Improving the physical realism and structural accuracy of protein models by a two-step atomic-level energy minimization. *Biophys. J.* 101, 2525–2534. doi: 10.1016/j.bpj.2011.10.024
- Xu, J., Wu, X. S., Sheng, J., Zhang, Z., Yue, H. Y., Sun, L., et al. (2016). -Synuclein mutation inhibits endocytosis at mammalian central nerve terminals. *J. Neurosci.* 36, 4408–4414. doi: 10.1523/jneurosci.3627-15.2016
- Yan, Y., Zhang, D., Zhou, P., Li, B., and Huang, S. Y. (2017). HDock: a web server for protein-protein and protein-DNA/RNA docking based on a hybrid strategy. *Nucleic Acids Res.* 45, W365–W373.
- Zhou, Y., Zhou, B., Pache, L., Chang, M., Khodabakhshi, A. H., Tanaseichuk, O., et al. (2019). Metascape provides a biologist-oriented resource for the analysis of systems-level datasets. *Nat. Commun.* 10: 1523.
- Conflict of Interest:** The authors declare that the research was conducted in the absence of any commercial or financial relationships that could be construed as a potential conflict of interest.
- Copyright © 2020 Kumar, Donakonda, Müller, Bötzel, Höglinger and Koeglsperger. This is an open-access article distributed under the terms of the Creative Commons Attribution License (CC BY). The use, distribution or reproduction in other forums is permitted, provided the original author(s) and the copyright owner(s) are credited and that the original publication in this journal is cited, in accordance with accepted academic practice. No use, distribution or reproduction is permitted which does not comply with these terms.